Mount Aragats as a stable electron accelerator for atmospheric high-energy physics research

Ashot Chilingarian,[1,2] Gagik Hovsepyan,[1] and Eduard Mnatsakanyan[1]

[1]*A. Alikhanyan National Lab (Yerevan Physics Institute), Alikhanyan Brothers 2, Yerevan 0036, Armenia*
[2]*National Research Nuclear University MEPhI (Moscow Engineering Physics Institute), Moscow 115409, Russian Federation*

(Received 28 September 2015; published 7 March 2016)

Observation of the numerous thunderstorm ground enhancements (TGEs), i.e., enhanced fluxes of electrons, gamma rays, and neutrons detected by particle detectors located on the Earth's surface and related to the strong thunderstorms above it, helped to establish a new scientific topic—high-energy physics in the atmosphere. Relativistic runaway electron avalanches (RREAs) are believed to be a central engine initiating high-energy processes in thunderstorm atmospheres. RREAs observed on Mount Aragats in Armenia during the strongest thunderstorms and simultaneous measurements of TGE electron and gamma-ray energy spectra proved that RREAs are a robust and realistic mechanism for electron acceleration. TGE research facilitates investigations of the long-standing lightning initiation problem. For the last 5 years we were experimenting with the "beams" of "electron accelerators" operating in the thunderclouds above the Aragats research station. Thunderstorms are very frequent above Aragats, peaking in May–June, and almost all of them are accompanied with enhanced particle fluxes. The station is located on a plateau at an altitude 3200 asl near a large lake. Numerous particle detectors and field meters are located in three experimental halls as well as outdoors; the facilities are operated all year round. All relevant information is being gathered, including data on particle fluxes, fields, lightning occurrences, and meteorological conditions. By the example of the huge thunderstorm that took place at Mount Aragats on August 28, 2015, we show that simultaneous detection of all the relevant data allowed us to reveal the temporal pattern of the storm development and to investigate the atmospheric discharges and particle fluxes.

DOI: 10.1103/PhysRevD.93.052006

I. INTRODUCTION

The theoretical investigation of the high-energy processes in the atmosphere was started 90 years ago by the Nobel Prize winner and creator of one of the first particle detectors C. T. R. [1]. Numerous papers published in recent decades by Gurevich, Dwyer, Babich, Lidvansky and coauthors (see citations to original publications in [2]) introduced the runway breakdown (RB), otherwise cited as relative runaway electron avalanches (RREAs) as a central engine of the high-energy processes in thunderstorm atmospheres. Measurements of particle fluxes on high mountains and in regions of Japan with low charge centers in thunderclouds prove the existence of particle fluxes that last up to a few tens of minutes correlated with thunderstorm activity (see details and references to original publications in the review of [3]). The first detection of huge fluxes of electrons, gamma rays, and neutrons on Mount Aragats in 2009 ([4]) has unambiguously established a new physical phenomenon—thunderstorm ground enhancement (TGE), increased fluxes of electrons, gamma rays, and neutrons detected by particle detectors located on the Earth's surface. The *in situ* observation of RREAs during the strongest thunderstorms on Aragats ([5]) and simultaneous measurements of TGE electrons and gamma-ray energy spectra ([6]) proved that RREA is a realistic and robust mechanism for electron acceleration in the atmosphere. These publications emphasized that lightning and TGEs are alternative mechanisms for the discharging of the atmospheric "electric engine"; they also introduced the origin of the highest energy gamma photons—modification of the cosmic-ray (CR) electron energy spectrum (MOS) in the strong electric field of the thundercloud. In [7], emphasized the role of the transient lower positive charge region (LPCR) in electron–gamma ray avalanche unleashing. Detailed measurements of the gamma-ray energy spectra by large NaI spectrometers on Aragats ([8]) allow us to reliably extend the energy range of the "thunderstorm" gamma rays up to 100 MeV. All these results were obtained at the Aragats research station in Armenia during the last 5 years with the "beams of the electron accelerator" operating in thunderclouds above the research station. The Aragats Space Environmental Center (ASEC, [9]) is located at an altitude of 3200 m on the plateau near a large lake and clouds usually form just above it (see Fig. 1).

Numerous particle detectors and field meters are located in three experimental halls as well as outdoors; the facilities are operated all year round. After understanding the TGE physics, we plan to apply this new evidence, i.e., fluxes of particles from the thundercloud, to approach the long-standing problems of lightning initiation and lightning leader propagation.

 © 2016 American Physical Society

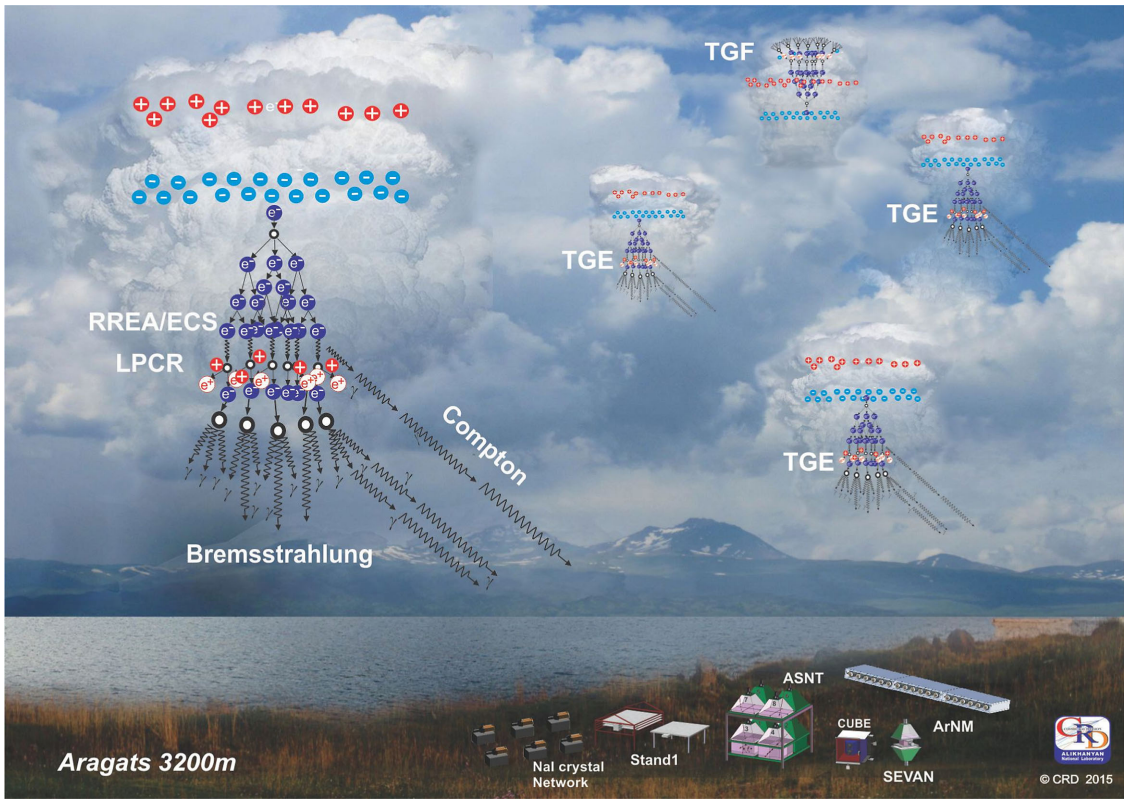

FIG. 1. Artistic view of the multiple RREA cascades in the thunderstorm atmosphere directed to Earth's surface (TGEs) and to space (TGF).

All the relevant information is being gathered, including data on particle fluxes, fields, lightning occurrences, and meteorological conditions. By the example of the huge thunderstorm that took place at Mount Aragats on August 28, 2015, we show that simultaneous detection of all the relevant data allowed us to reveal the temporal pattern of the storm development and to investigate the atmospheric discharges and particle fluxes. The paper is comprised of the following sections: instrumentation; chain of positive lightning strikes; chain of negative lightning strikes; small size TGE; and large size TGE. Thunderstorms are very frequent above Aragats, with peak activity in May–June and September–October. Almost all of them are accompanied with enhanced particle fluxes. In Fig. 1 we see an artistic view of multiple electron–gamma ray avalanches directed to the Earth's surface and to open space. The first ones originated TGEs registered by the ground-based particle detectors; the second ones originate from terrestrial gamma flashes (TGFs) ([10]) observed by the orbiting gamma-ray observatories.

By analyzing a particular stormy day at Aragats, namely, August 28, 2015, we will demonstrate the operation of the electron "accelerator" in the vicinity of the station and present the stages of our physical inference on the discovery of the new phenomenon of "long TGEs"—enhancements of low-energy gamma-ray fluxes (0.4–2 MeV) that last for several hours.

II. INSTRUMENTATION

The particle detectors of the Aragats Space Environmental Center (ASEC) ([9]) can measure the fluxes of the species of secondary cosmic rays (electrons, gamma rays, muons, and neutrons), which have different energy thresholds. Numerous thunderstorm-correlated events, detected by the ASEC facilities, constitute a rich experimental set for the investigation of the high-energy phenomena in the thunderstorm atmosphere. The new generation of ASEC detectors consist of 1- and 3-cm-thick molded plastic scintillators arranged in stacks and cubic structures. The "STAND1" detector is comprised of three layers of 1-cm-thick, 1-m^2 sensitive area molded plastic scintillators fabricated by the High Energy Physics Institute, Serpukhov, Russian Federation; see Fig. 2. The light from the scintillator through optical spectrum-shifter fibers is reradiated to the long-wavelength region and passed to the photomultiplier FEU-115M. The maximum of luminescence is emitted at the 420-nm wavelength, with a luminescence time of about 2.3 ns. The STAND1 detector is tuned by changing the high voltage applied to photomultiplier (PM) and setting the thresholds for the discriminator shaper.

The threshold should be chosen to guarantee both high efficiency of signal detection and maximal suppression of photomultiplier noise. Proper tuning of the detector provides ~99% efficiency of charged particle detection. The data

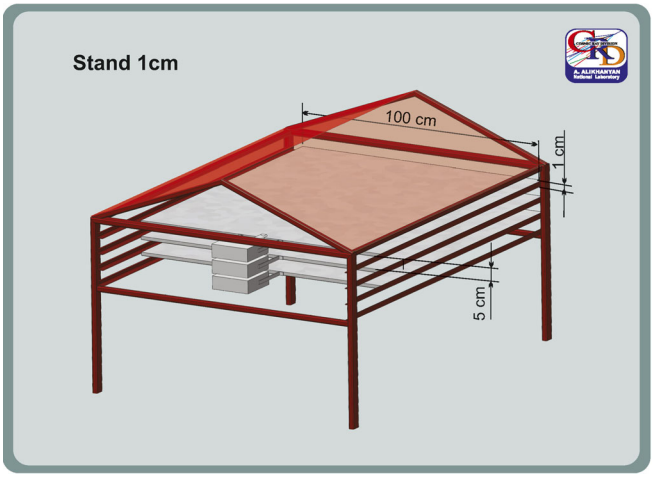

FIG. 2. STAND detector consisting of three layers of 1-cm-thick scintillators.

acquisition (DAQ) system counts and stores all coincidences of the detector channels. Coincidence "100" means that a signal has been registered in the upper detector only. This combination registered low-energy electrons with an efficiency of ∼99%; the threshold energy of ∼1 MeV is one of the lowest among all ASEC detectors. The gamma-ray detecting efficiency of this combination is about 2%. For the coincidence 010, the gamma ray detection efficiency is increased to ∼3% due to creation of the additional electron-positron pairs in the substance of the upper scintillator. Coincidence "111" means that all three layers register particles; the minimal energy of charged particles giving a signal in all three layers is ∼10 MeV. With the same DAQ electronics are registered the time series of a similar (but 3-cm-thick) particle detector stand near the stacked structure.

Special experimental facilities were designed and installed at Aragats in order to separate electron and gamma-ray fluxes. Two 20-cm-thick plastic scintillators are surrounded by 1-cm-thick molded plastic scintillators (see Fig. 3). Thick scintillators detect charged flux with a very high efficiency (∼99%); they can also detect neutral flux with an efficiency of ∼20%. Thin scintillators also detect charged flux with very high efficiency (∼99%), though the efficiency of detecting neutral flux is highly suppressed and equals 1%–2%. Thus, using the coincidences technique, it is possible to purify the neutral flux detected by inside scintillators, rejecting the charged flux by the veto signals from surrounding thin scintillators. The calibration of the cube detector proves that the veto system (preventing the counting signal in the thick scintillator if there is a signal in at least one of the six surrounding thin scintillators) can reject 98% of the charged flux (see details in [6]).

The histograms of the energy deposits in the two inner thick scintillators are stored every minute. The one-minute count rates of the surrounding 6 scintillators are measured and stored as well.

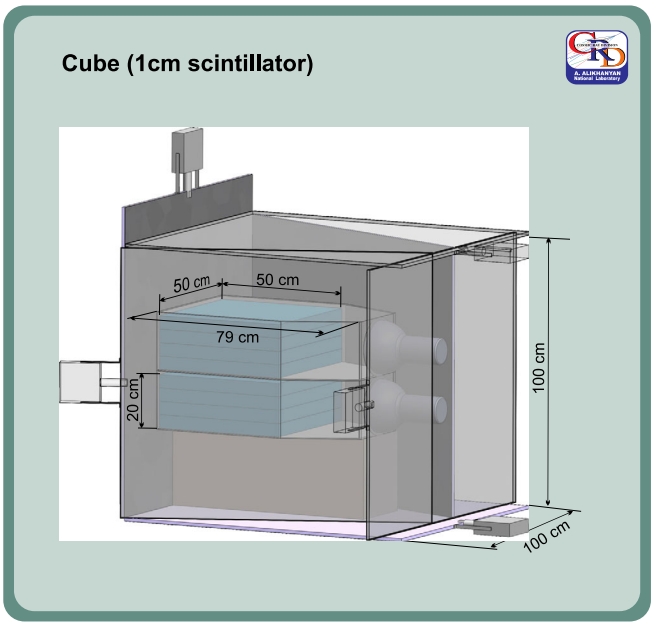

FIG. 3. CUBE detector. The thick scintillators located inside are measuring neutral flux with purity ∼98%.

The detector network measuring particle energy consists of four NaI crystal scintillators packed in a sealed 3-mm-thick aluminum housing. The NaI crystal is coated by 0.5 cm of magnesium (MgO) by all sides (because the crystal is hygroscopic) with a transparent window directed to the photo-cathode of a FEU-49 PM; see Fig. 4.

The large cathode of FEU-49 (15-cm diameter) provides a good light collection. The spectral sensitivity range of FEU-49 is 300–850 nm, which covers the spectrum of the light emitted by NaI(Tl). The sensitive area of each NaI crystal is ∼0.0348 m^2, the total area of the four crystals is ∼0.14 m^2, and the gamma-ray detection efficiency is ∼80%. A logarithmic analog-digit converter (LADC) is used for the coding of PM signals. Calibration of LADC

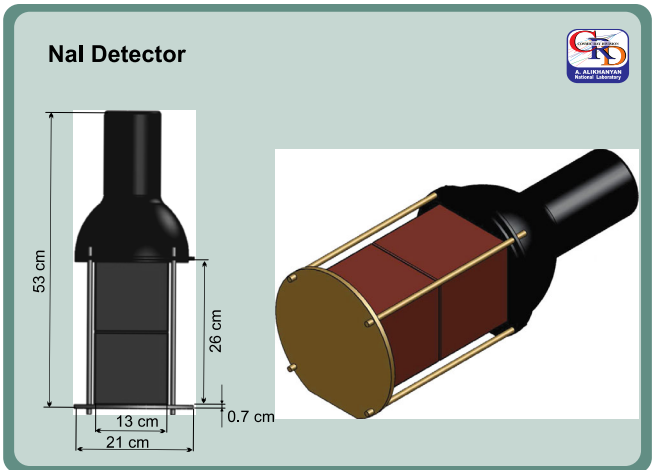

FIG. 4. NaI(Tl) crystal assembly.

and code-energy conversion was made by detecting the peak from exposed ^{137}Cs isotope emitting 662 keV gamma rays and by the high-energy muon peak (55 MeV) in the histogram of energy releases in the NaI crystal. The PM high voltage was tuned to contain both structures (peaks) in the histogram of LADC output signals (codes) and to ensure linearity of LADC in the energy region of 0.4–60 MeV. A detailed description of other ASEC detectors, including charts with all sizes, is available from the WEB site of the Cosmic Ray Division of Yerevan Physics Institute http://crd.yerphi.am/ADEI in the WIKI section of the multivariate visualization platform and from ([4,11]).

The count rate of a particle detector depends on the chosen energy threshold of the shaper discriminator, the size of the detector, and the amount of matter above it. The inherent discrepancy of the parameters of PMs also can add ∼15% difference to the particle detector count rates. A significant amount of substance above the sensitive volume of NaI crystals (0.7 mm of roof tilt, 3 mm of aluminum, and 5 mm of MgO) prevents electrons with energy lower than ∼3 MeV from entering the sensitive volume of the detector. Thus, the network of NaI spectrometers below 4 MeV can detect gamma rays only.

The small sizes of the NaI crystals and short duration of TGE pose a limitation on the lowest gamma-ray flux that can be reliably observed. The usual requirement on the minimal amount of particles in a histogram bin is >5; therefore, the minimal flux that can be reliably detected by the NaI network should be above 200 per minute per m^2 (the area of four crystals is 0.14 m^2 and the required number of particles in four crystals is greater than 20). For smaller fluxes, fluctuations overwhelm the signal.

The significance of detecting peaks in the time series of the particle count rates is determined by the p-values of the peak significance test, i.e., by the value of the peak divided by the standard deviation of the count rate (number of standard deviations contained in the peak, Nσ). The p-value is the most comprehensive measure of the reliability of detecting peaks in a time series. A large p-value corresponds to small-chance probabilities that the observed peak is a background fluctuation and not a genuine signal. Therefore, we can safely reject the null hypothesis (background fluctuation) and confirm the TGE. Very large p-values not only prove the unambiguous existence of a particle flux from the cloud, but also serve as a comparative measure of the TGE observations using different detectors.

The deep negative near-surface electric field is a necessary condition for the TGE origination. Moreover, the observed changes of the electric field, along with detected particle fluxes, encompass information on the dynamics of the cloud electrification, which is very difficult to acquire by *in situ* measurements. A network of three electric mills continuously monitors the disturbances of the electric field on Mount Aragats. The electrical mill EFM 100 produced by the Boltek Company operates with a 20-Hz frequency, performing 20 measurements of the near-surface electric field per second. Comparisons of electric field strengths obtained by the three identical EFM-100 electrical mills prove the reliability and high accuracy (discrepancy of device readings do not exceed 10%) of electric field measurements.

III. SERIES OF POSITIVE LIGHTNINGS AT ∼12:00–13:00

On August 28, almost all day long, the thunderstorms at Aragats were accompanied with numerous nearby lightning strikes and several episodes of the enhanced particle fluxes registered by the detectors located at ASEC.

The network of NaI spectrometers had detected an enhanced flux of low-energy gamma rays with several

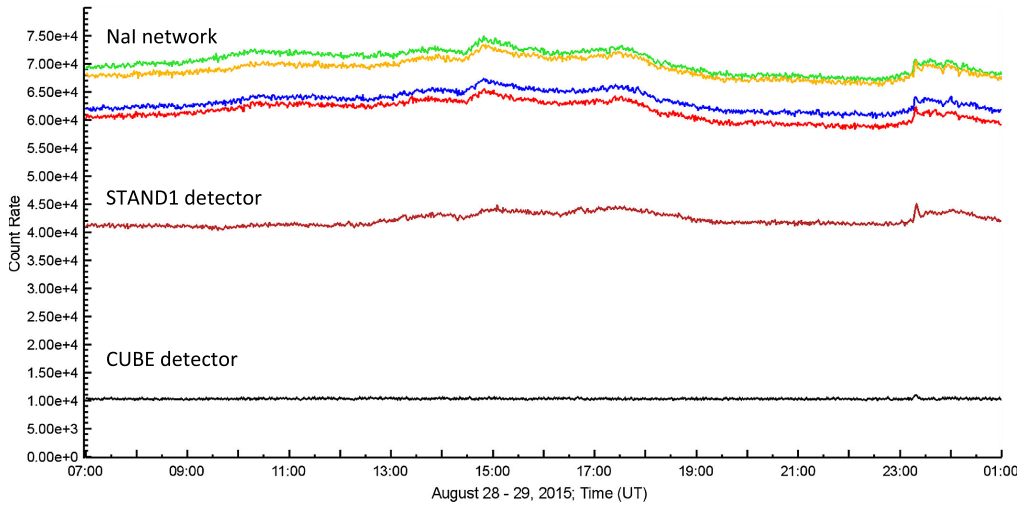

FIG. 5. One-minute count rates of the network of four NaI spectrometers. TGE at 23:18–23:21 contains high-energy gamma rays detected by all ASEC particle detectors.

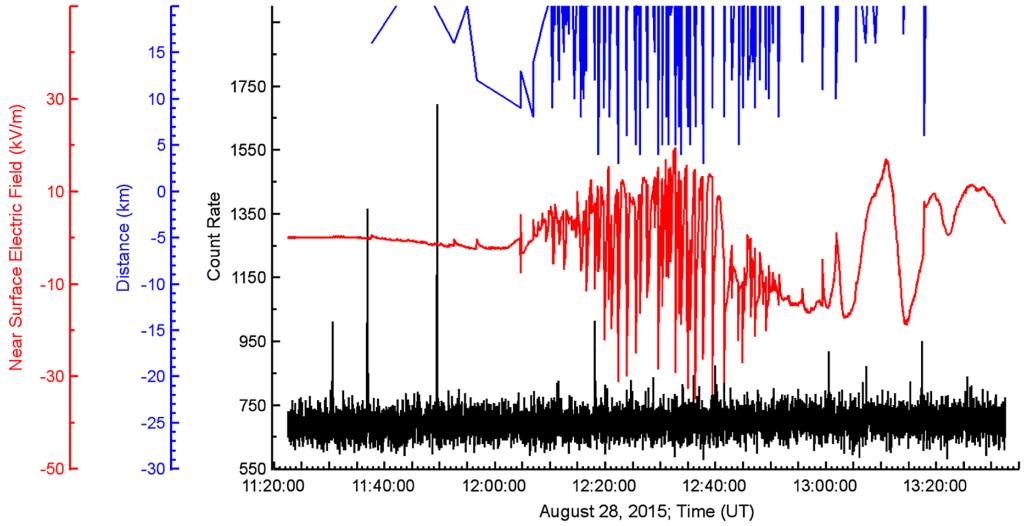

FIG. 6. Positive lightning series observed on August 28, 2015, 12:00–13:00. The top lines show distance to lightning, the middle curve shows disturbances of the near-surface electric field, and the bottom shows the 1-second time series of count rates of the 3-cm-thick, 1-m^2 area plastic scintillator.

episodes of abrupt bursts, as shown in Fig. 5. In spite of the fact that the NaI crystals are much smaller than the plastic scintillators, due to the low-energy threshold (0.4 MeV) and higher efficiency to register gamma rays the count rates of each of the four spectrometers are higher than the counts of larger plastic scintillators. The ∼15% discrepancy of the count rates of the four spectrometers is explained by the differences in PM parameters. This discrepancy does not influence the amplitude of TGE (peak value of the count subtracted by background value), which is the same for all four spectrometers. The matter above the sensitive volume of NaI spectrometer absorbs electrons with energies below 3 MeV; the detection of electrons and gamma rays of higher energy is possible. In Fig. 5 we can see that the time series of the CUBE detector (a 20-cm-thick detector located inside the veto housing with energy threshold ∼4 MeV) demonstrates enhancement only around 23:20 when, as we will see later, the gamma-ray flux exceeded 4 MeV due to presence of the bremsstrahlung gamma rays from the runaway electrons. The STAND1 detector (energy threshold ∼1 MeV) showing a flux enhancement coherent to NaI at a smaller scale had also demonstrated a pronounced peak around 23:20.

For recovering electron and gamma-ray intensity in the TGE flux at energies above 4 MeV we use data from the CUBE detector, vetoing the charge flux.

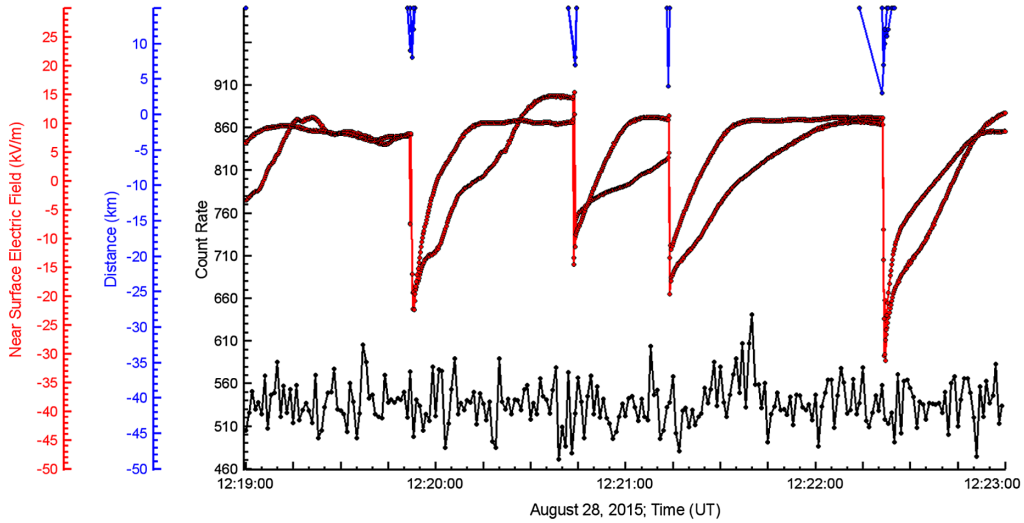

FIG. 7. One episode of positive lightning series observed on August 28, 2015, at 12:00–13:00. The top lines show distance to lightning, the middle two curves show disturbances of the near-surface electric field measured by electric mills located at a distance of 300 m from each other, and the bottom shows the 1-second time series of count rates of the 3-cm-thick, 1-m^2 area plastic scintillator.

TABLE I. Main characteristics of a sample of lightning occurrences at 12:19–12:23 on August 28, 2015.

Start of lightning (UT) and el. field value (kV/m)	Time of el. field minimum (UT) and field minimal value (kV/m)	Duration (sec)	Recovering (sec)	Drop of el. field	Dist. (km)	WWLLN time	WWLLN dist.
12:19:52.1 8	12:19:52.75 -23	0.65	21	−31	8		
12:20:43.7 15	12:20:43.8 -18	0.1	29	−33	7		
12:21:13.8 10	12:21:14.0 -20	0.2	23	−30	4		
12:22:21.3 10	12:22:21.8 -30	0.5	31	−40	3		
12:51:31.15 -14	12:51:31.55 -8	0.4	29	6	8	12:51:31.23–12:51:31.47	5–9

Due to the small sensitive area of NaI spectrometers, we can recover differential energy spectra at energies above $\sim 10^3/\mathrm{m}^2$ min, equivalent to 5–10 registered particles in an energy bin. Histograms of the energy releases in NaI crystals are collected and stored each minute; therefore we can recover 1440 energy spectra daily. To achieve better statistical accuracy, we use the data from all four spectrometers and combine several minutes around the peak values of the count rate. The energy spectra were recovered, according to the methodology described in ([12]), for four TGE episodes at 14:49–14:52, 16:37–16:44, 23:18–23:21, and 23:29–23:31. The relative enhancement was calculated by subtracting from the peak value of the count rates the background measured just before the enhancement started. Only the relative enhancement in measurements with NaI crystals has physical meaning in the described series of measurements. The NaI spectrometers were located just below the iron tilts of the roof. In August at Aragats, the sun is extremely strong and the temperature under the iron roof reached 50–60 C°. The high temperature influenced DAQ electronics and, respectively, the detector count rate increased at peak temperatures up to 10% as compared with nighttime count rate when the temperature drops down to 5–10 C°. Therefore, though the maximal absolute count rate was achieved at ∼15:00, the TGE at 23:20 has larger amplitude and was much more significant; it could be explained by the bremsstrahlung gamma rays emitted by the runaway electrons in the thundercloud just above the detectors.

The electric field disturbances on August 28, 2015, were prolonged and deep, reaching −35 kV/m; lightning activity was strong and some of the lightning strikes were within 5 km of the station. Numerous positive lightning strikes that started at ∼8:00 stipulate small disturbances of the near-surface electric field. The network of three EFM-100 electric mills measured the near-surface electric field. The devices operated according to the "atmospheric electricity" sign convention (a positive electric field at ground is produced by positive charge overhead and negative electric field on the ground is produced by negative charge overhead). Thus, the recorded positive field change corresponds to negative lightning, which decreases the negative charge overhead and negative field change corresponds to positive lightning, which decreases the positive charge overhead. The heavy-duty storm that started at ∼12:00 was followed by copious positive lightning strikes lasting until ∼13:00 (Fig. 6). In Fig. 6 we show the electric field disturbances measured by the electric mill located on the roof of the MAKET building, the corresponding distance to the lightning and one-second time series of 1-m^2 plastic scintillator. The spikes in the particle count rates are due to the showers hitting the scintillator. In one-minute time series they are smoothed by integration over 60 seconds, but in 1-second time series spikes are visible.

In Fig. 7 we show four minutes of stormy weather matched with four positive lightning strikes (zoomed from Fig. 6).

The pattern of rapid decrease of the electric field was approximately the same for both electric mills located at a distance ∼300 m from each other. The abrupt decrease of the near-surface electric field followed by relatively slow recovery indicates the neutralization of a positive charge in the thundercloud. However, the operation of the charging engine permanently recovers the positive charge region in the thundercloud. In Table I we post the characteristic of

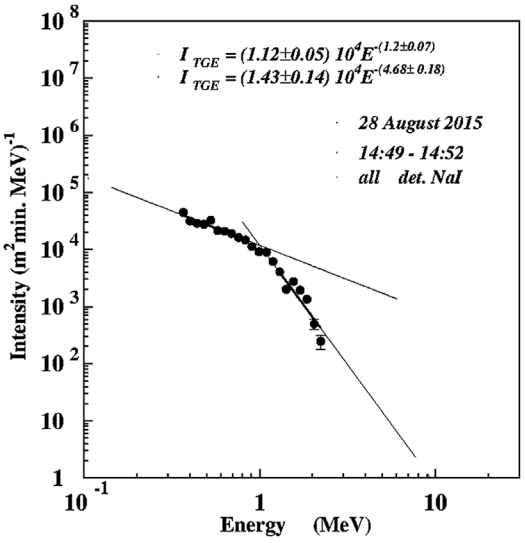

FIG. 8. The differential energy spectrum of the sum of 4 NaI spectrometers. The background was measured just before the TGE started. Flux intensity is $0.18 \times 105/\mathrm{m}^2$ min, knee position is 0.9 MeV, and intensity after knee is $0.50 \times 10^4/\mathrm{m}^2$ min.

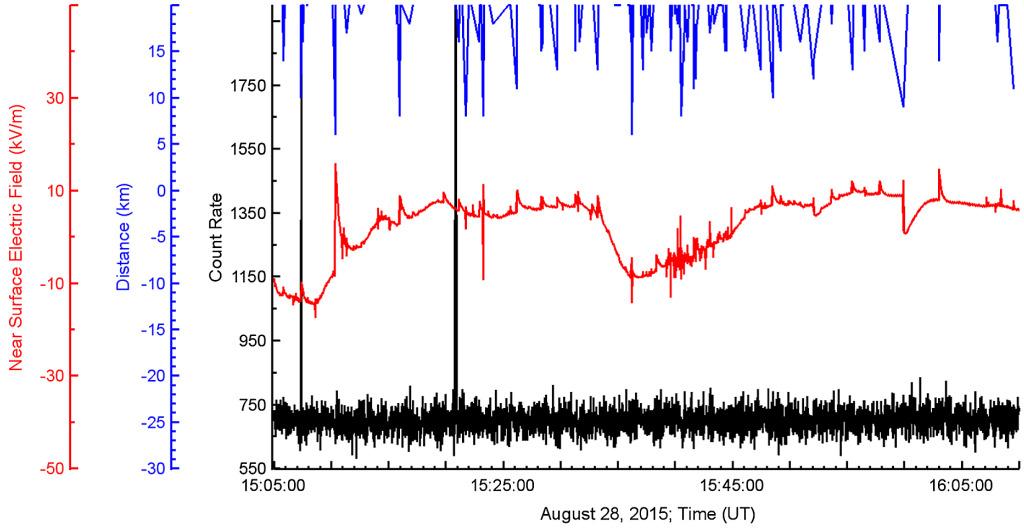

FIG. 9. Multiple negative lightning strikes detected at 14:45–16:30. The top lines show distance to lightning, the middle curve shows disturbances of the near-surface electric field, and the bottom shows 1-second time series of the count rates of the 3-cm-thick, 1-m^2 area plastic scintillator.

four positive (+CG) lightning strikes from ∼100 that occurred on August 28, 2015; at the end of an hour-long series of positive lightning strikes, they changed to the negative ones.

Although the amplitudes of negative lightning strikes were small, four strikes (at 12:51:31.23–12:51:31.47) were registered by the Worldwide Lightning Location Network (WWLLN), one of the nodes of which is installed at the Cosmic Ray Division (CRD) headquarters in Yerevan, ∼50 km from Aragats station.

From Table I, where we present the main characteristics of the lightning strikes shown in the previous figure we can outline typical features of the positive cloud-to-ground lightning that occurred on Aragats on August 28, 2015:

1. Mean electric field before the start of the lightning ∼8–15 kV/m;
2. Typical values of the drop of electric field ∼ − 30– − 40 kV/m;
3. After reaching its minimum, the near-surface electric field slowly returned to the prelightning values due to continuous charge separation processes in the cloud in 21–31 seconds;
4. Time from the start of electric field sharp decrease till its minimum was ∼0.1–0.65 sec;
5. Distance to lightning was ∼3–8 km.

The rather large amplitude of the positive lightning field changes (−30– − 40 kV/m) achieved in less than 1 sec and the large recovery time of electric field (tens of seconds) indicate strong discharge processes at nearby distances (10 km). Several high masts are located near the station; from their tops the electron streamers can propagate to the positive charge regions in the thunderclouds above. As usual during a series of positive lightning strikes no enhancements of particle flux were registered.

The strong rain that started at 13:22 stopped at 14:00. The temperature started to rise from 4 C° at 13:00 to 6 C° at 14:30 and then abruptly dropped to 3.4 C° at 14:50 UT. The relative humidity decreased from 95% at 13:00 to 75% at 14:30. The electric field was in the negative domain −8 to −24 kV/m; few lightning strikes were detected. At

TABLE II. Main characteristics of a sample of lightning occurrences at 15:38–16:03 on August 28, 2015.

Start of lightning (UT) and el. field value (kV/m)	Time of el. field maximum (UT) and field maximal value (kV/m)	Duration (sec)	Recovering (sec)	Drop of el. field	Dist. (km)	WWLLN time	WWLLN dist.
15:38:21.8 -7	15:38:22.7 -4	0.9	32	3	14	15:38:22.41	21
15:53:39.4 7	15:53:40.3 (15:53:39.9) 10	0.9	41	3	18	15:53:39.5	14
15:59:54.4 9	15:59:54.6 12	0.2	0.1	3	9	15:59:54.32	14
15:59:54.85 9	15:59:55.0 2	0.15	180	−7	20	15:59:54.34	8
16:03:01.05 8	16:03:01.55 15	0.5	27	7	13,15	16:03:01.0 – 16:03:01.86	11–21

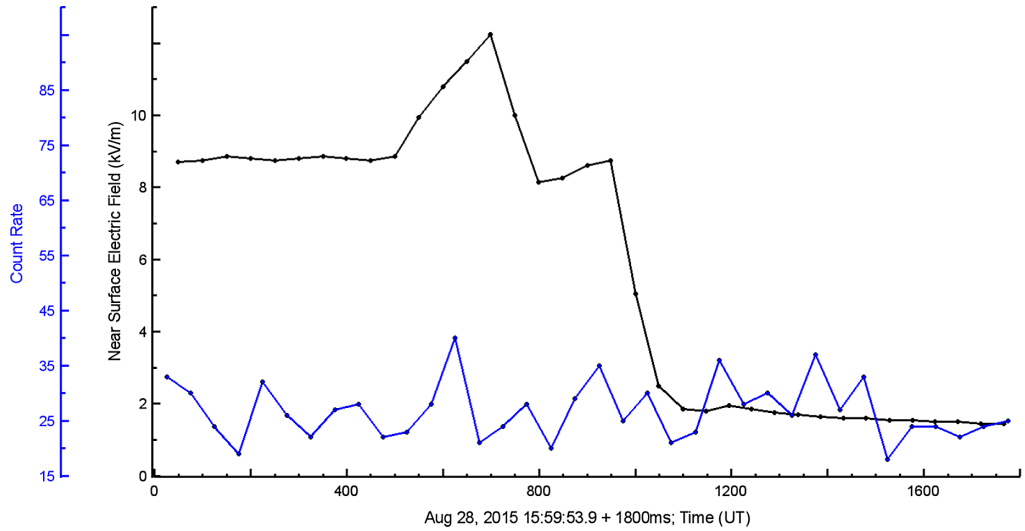

FIG. 10. Disturbance of the near-surface electric field when the negative discharge suddenly turned to a positive one. The bottom line shows the 50-m sec time series of the 3-cm-thick, 1-m^2 area, outdoor plastic scintillators.

14:30 the gamma-ray flux started to rise, reaching maximum at 14:50. The differential energy spectrum of the gamma-ray flux is shown in Fig. 8. We fit the energy spectrum with two power law dependences; the point where interpolating dependence changes is usually named the "knee." The knee position is located at ~1 MeV and is rather smooth. The energy spectrum extends to ~2 MeV and then quickly decays.

In the next hour the lightning activity became stronger; see Fig. 9. However, the atmospheric discharges were far from the Aragats station and, therefore, the amplitudes of the near-surface electric field disturbances were small, as shown in Table II. The relative humidity (RE) successively increased from 75% at 14:30 to 92% at 15:45 when the rain resumed. At the same time, the wind speed decreased from 2 m/ sec to 0.2–0.6 m/ sec and the temperature decreased from 3.4 C° to 2.9 C°.

IV. SERIES OF NEGATIVE LIGHTNING STRIKES AT ~15:00–16:00

After 15:00, as we can see from Fig. 9 and the Table II that the pattern of disturbances of electric field drastically changed as compared with the ones registered 2 hours before (Figs. 6 and 7). The lightning locations were 10–20 km from the station (confirmed by WWLLN; see the last column of Table II). Therefore, the amplitude of disturbances of the near-surface field was small, −3–7 KV/m. Lightning strikes were mostly negative; i.e., the large amount of negative charge overhead was decreased. No TGEs were detected. The spike in 1-sec time series of the plastic scintillator was due to the particle shower that hit the detector at 15:07:23.

The illustration of the 3 seconds of time series of the near-surface electric field, revealing the pattern of an unusual lightning strike that occurred at 15:59:54.4–15:59:55, is given in Fig. 10. In 0.6 seconds the negative discharge (abrupt enhancement of the electric field) with amplitude 3 kV/m suddenly turned to a positive one (abrupt decrease of the electric field) with amplitude −7 kV/m (see also Table II).

V. SMALL SIZE TGE WITH MAXIMUM AT ~16:40

At 16:20 the electric field moved to a negative domain and at 16:43 it dropped to −23 kV/m. Between 16:36 and 16:43 at the large negative electric field several small "bumps" appeared with an amplitude less than 5 kV/m. During that "bumpy" time (16:37–16:44) several ASEC

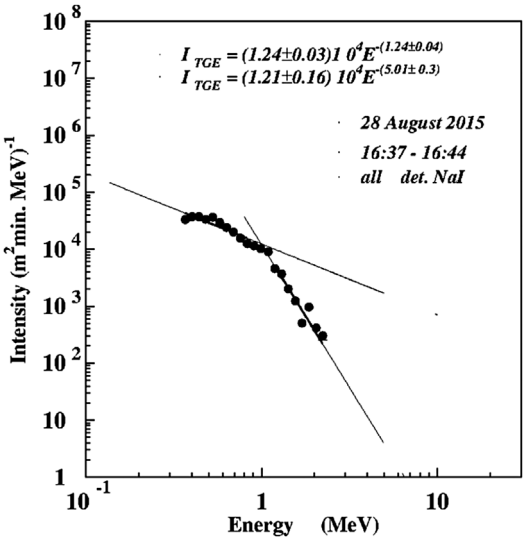

FIG. 11. Differential energy spectrum of the "small size" TGE. Flux intensity is $0.95 \times 10^4/m^2$ min, knee position is 0.9 MeV, and intensity after knee is $0.25 \times 10^4/m^2$ min.

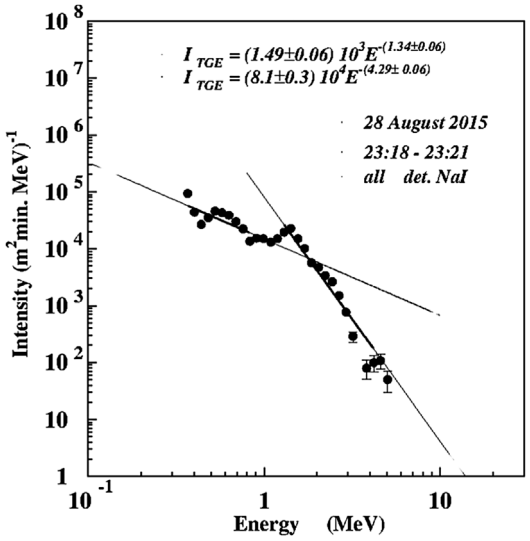

FIG. 12. Differential energy spectrum of TGE obtained by the 4 NaI spectrometers: flux intensity is $0.34 \times 10^5/\mathrm{m}^2$ min, knee position is 1.2 MeV, and intensity after knee is $0.17 \times 10^5/\mathrm{m}^2$ min.

particle detectors registered TGE. The intensity of the event was two times less than previous TGE; see Fig. 11. The knee position is analogous to the previous spectrum and the change of the interpolating power law function is smooth too. The energy spectrum continues to ∼2 MeV.

The relative humidity (RE) was 92–95% during TGE (high RE is another necessary condition to unleash large TGE) and wind speed was ∼1 m/ sec. The temperature started to fall at 16:26 from 3.5 C° down to 2.9 C° during TGE. Wind direction was 180°N. It stopped raining at 16:27 and resumed at 17:00. Consequently, there was no rain during TGE.

VI. LARGE TGE OCCURRED AT ∼23:18–23:21

Disturbances of the electric field and lightning strikes took place until 17:30 and the rain did not stop until 22:00. After the rain stopped, the electric field started to decrease at 23:00 reaching −28 kV/m at 23:21. The relative humidity (RE) went up from 89% at 23:14 to 92% at 23:17 and remained there until 23:23. Wind speed abruptly increased from 0 m/ sec at 23:13 to 7.5 m/ sec at 23:19, and then decreased down to 1 m/ sec at 23:23. The temperature started to decrease at 23:13 from 3.9 C°, reaching 0.8 C° at 23:23. Wind direction was 200N. The TGE flux reached maximum at 23:19; energy spectra of TGE extended to 6 MeV (see Fig. 12). The TGE event duration was ∼10 minutes; intensity and maximal energy were greatest on August 28. Knee position shifted to 1.2 MeV and the knee was sharper than in previous TGEs. The intensity of TGE is the highest among those observed on August 28, 2015.

The veto system of the CUBE detector rejected most of the charged particles by six 1-cm-thick plastic scintillators with 1-m^2 area shaped in a cubic structure. The two 20-cm thick scintillators located inside an area of 0.25 m^2 registered neutral particles with the veto system switched on. The CUBE detector with two inner 20-cm-thick plastic scintillators with energy threshold ∼4 MeV also demonstrated pronounced peaks (Fig. 13). Figure 13 does not show the time series of the count rates itself, but the time series of the p-values of the peak significance test. The large p-values of peaks observed by the two inner 20-cm-thick scintillators of the CUBE detector allows us to estimate charged and neutral fluxes of TGE above ∼4 MeV (NaI spectrometers allow us to measure pure gamma-ray flux below 3–4 MeV and mixed flux above 3–4 MeV).

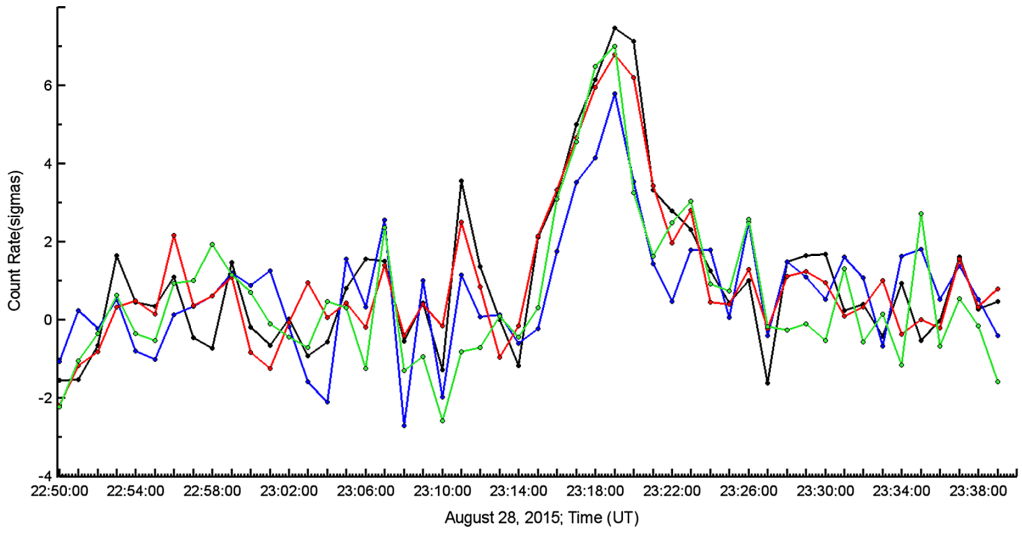

FIG. 13. TGE observed by the CUBE detector's two stacked 20-cm-thick plastic scintillators with and without the veto system switched on.

TABLE III. Count rate of 20 cm thick plastic scintillator with and without veto (minutes after 23:00 UT).

August 28 (UT)				
23:16	10548	8614	4526	3577
23:17	10736	8749	4633	3647
23:18	10853	8797	4735	3739
23:19	**10990**	**8923**	**4802**	**3764**
23:20	10954	8750	4755	3585
23:21	10564	8589	4534	3507
23:22	10508	8516	4418	3548
23:23	10459	8617	4484	3575

From Table III we can see that at 23:19 the CUBE scintillators registered maximal count rate; for that minute we calculate the electron and gamma-ray intensities incident on the CUBE detractor.

Due to a nonzero probability of electrons to miss registration in the 1-cm-thick plastic scintillator of the veto system, and due to a nonzero probability for the detection of the gamma ray by the same scintillator, we have made corrections to recover intensities (see details in [6]). However, these corrections are below ∼2% as compared with calculation of the gamma-ray intensity directly from the amplitude of the peak observed by the thick scintillator with the veto switched on (538 counts). The intensity of gamma rays above ∼4 MeV is $\sim 10^4/\mathrm{m}^2$ min, and the intensity of electron flux is $-8 \times 10^2/\mathrm{m}^2$ min. Thus, the fraction of electrons at energies above 4 MeV does not exceed ∼7%.

In Table IV we show the mean values of count rate, the peak value, amplitudes of the peaks (also in the number of standard deviations), and calculated intensities (integral spectra) of gamma-ray and electron flux above ∼4 MeV. We assume the efficiency of gamma-ray detection by the 20-cm-thick scintillator to be equal to 20% and detection of electrons 99%.

The efficiency of detecting gamma rays by the "veto" 1-cm-thick scintillators is 2% and electrons 99%. Particles to be registered in the bottom thick scintillator (see Fig. 3) should traverse through the upper one; therefore due to attenuation of the particle flux, intensities measured by the bottom scintillator are significantly lower.

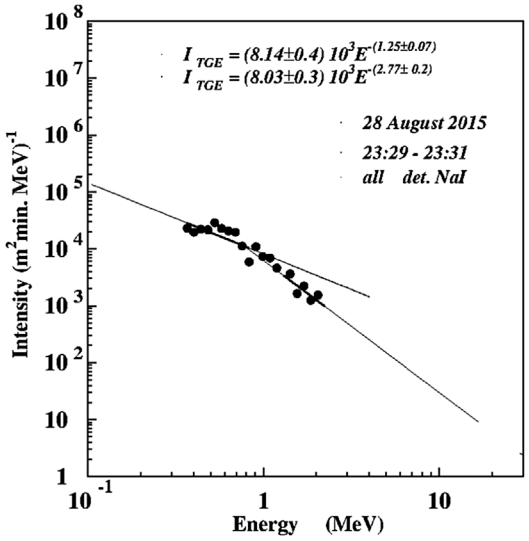

FIG. 14. The differential energy spectrum of the sum of the 4 NaI spectrometers measured after large TGE. Entire intensity is $0.21 \times 10^5/\mathrm{m}^2$ min, knee position is 1.2 MeV, and intensity after knee $0.4 \times 10^4/\mathrm{m}^2$ min.

After the decline of TGE at 23:23 the low-energy particle flux measured by NaI spectrometers remained high. However, the conditions required for unleashing large TGE did not last and the energy spectrum measured at 23:39–23:41 contained only low-energy particles (see Fig. 14).

VII. DISCUSSION AND CONCLUSIONS

The model of TGEs can be formulated briefly as follows ([13]): electrons from the ambient population of cosmic rays (CR) are accelerated downward (towards the Earth) by the positive dipole formed by the main negatively charged layer in the middle of the cloud and a transient lower positive charge region in the bottom of the cloud. In very strong electric fields, the energy gained from the field surpasses the electron energy losses in the atmosphere and the intensive process of the electron multiplication and acceleration initiate large particle avalanches reaching and being registered on the Earth's surface (TGE). If the strength of the electric field is not enough to start RREA, nonetheless the energy of an electric field is transferred to

TABLE IV. Calculated intensities of TGE electron and gamma-ray fraction; threshold 4 MeV.

Name	Mean	σ	23:19 peak	TGE–ΔN (Nσ)	e intensity ($1/\mathrm{m}^2$ min)	γ intensity ($1/\mathrm{m}^2$ min)	e/γ
Cube 7	10258	108	10990	742 (6.9)	800	10920	7.3%
Cube 8	8494	81	8923	429 (5.3)	368	6768	5.4%
7 with veto	4294	79	4802	538 (6.8)	not applicable	not applicable	not applicable
8 with veto	3431	47	3764	333 (7.1)	not applicable	not applicable	not applicable

the electrons, changing their energy spectrum and enhancing the probability of bremsstrahlung (MOS process). Both MOS and RREA processes have been experimentally observed at Aragats high-mountain research station in good agreement with simulations ([6]). Recently as well intense fluxes of gamma rays were measured by the airborne detector near the end of a downward RREA, consistent with another positive dipole occurring between the main positive charge layer and the negative screening layer above it (the authors named them "gamma glows" [14]).

However, in our previous publications we consider TGE events, mostly large ones, when the RREA was unleashed just above the detector site during several minutes. In this paper, we consider data collected on a whole day of August 28, 2015. The day was stormy, electric field disturbances continuous, lightning strikes enormous, and the electron accelerator above provided evidence on several long, low-energy TGEs and intensive and energetic enhancements. For the first time we describe and analyze not only isolated TGE events, but also the whole temporal history of the long duration thunderstorm, including high- and low-energy TGEs, periods of positive and negative lightning strikes, meteorological conditions, and disturbances of the near-surface electric field. By scrutinizing a particular stormy day at Aragats we demonstrate operation of the "moving electron accelerator" generated high-energy (up to 6 MeV) bremsstrahlung gamma photons when RREA is above the station and low-energy (0.4–2 MeV) Compton-scattered gamma rays when a strong electric field moved several kilometers away from the station.

NaI spectrometers registered an additional (compared to the fair weather day) ∼1.8 million gamma rays in total. TGE differential energy spectra were estimated by the network of the NaI spectrometers for 4 TGE episodes. Three of them contained only low-energy gamma rays with energies below 2 MeV; large TGE with maximal flux at 23:19 also contain gamma rays with energies up to 6 MeV. The spectrometer data are confirmed by the count rate measurements of other ASEC detectors. The 1-minute time series of the CUBE detector with an energy threshold above ∼4 MeV does not demonstrate any enhancements for the low-energy TGEs. The same time series demonstrates pronounced peaks with very high statistical significance for the high-energy TGE. The energy spectra are of a broken power law type. Due to the very large number of registered gamma rays we estimate spectra for each of the TGE events. We fit our spectra with two power law dependences that allow physical inference on the possible origin of two gamma-ray populations. According to the model of TGE initiation ([13]) the intense RREA process in the cloud originates bremsstrahlung photons that follow the passage of electrons. The electrons from the ambient population of secondary cosmic rays were accelerated up to energies 30–40 MeV. The size of LPCR does not extend more than 1 km; therefore high-energy bremsstrahlung photons illuminate the Earth's surface only locally under the thundercloud. The Compton-scattered photons of lower energy due to much broader angular distribution can illuminate a much larger surface under a cloud. Only on a few occasions when LPCR is above the detector site do we register large TGE with maximal energies above 3–4 MeV. These episodes are usually short because the wind moves the cloud relative to the particle detector location. The Compton scatter photons can reach the detector site from several RRE avalanches periodically emerging in the large thundercloud for the much longer time; see Fig. 1. The position of the knee at 1.2 MeV supported our assumption. The intensity of the gamma rays with energies above the pair production threshold (1.022 MeV) should be abruptly decreased due to catastrophic energy losses of the electrons and positrons in the atmosphere.

ACKNOWLEDGMENTS

The authors thank the staff of the Aragats Space Environmental Center for the uninterruptible operation of Aragats research station facilities. The data for this paper are available via the multivariate visualization software ADEI on the Web page of the Cosmic Ray Division (CRD) of the Yerevan Physics Institute [15]. The authors wish to thank the World Wide Lightning Location Network [16], a collaboration among more than 50 universities and institutions, for providing the lightning location data used in this paper. The research was supported by the Armenian Government Grant 15T-1C011.

[1] C. T. R. Wilson, The acceleration of β-particles in strong electric fields such as those of thunderclouds, Proc. Cambridge Philos. Soc. **22**, 534 (1925).

[2] J. R. Dwyer, D. M. Smith, and S. A. Cummer, High-energy atmospheric physics: Terrestrial gamma-ray flashes and related phenomena, Space Sci. Rev. **173**, 133 (2012).

[3] J. R. Dwyer and M. A. Uman, The physics of lightning, Phys. Rep. **534**, 147 (2014); J. R. Dwyer, D. M. Smith, and S. A. Cummer, High-energy atmospheric physics: Terrestrial

gamma-ray flashes and related phenomena, Space Sci. Rev. **173**, 133 (2012).
[4] A. Chilingarian, A. Daryan, K. Arakelyan, A. Hovhannisyan, B. Mailyan, L. Melkumyan, G. Hovsepyan, S. Chilingaryan, A. Reymers, and L. Vanyan, Ground-based observations of thunderstorm-correlated fluxes of high-energy electrons, gamma rays, and neutrons, Phys. Rev. D **82**, 043009 (2010).
[5] A. Chilingarian, G. Hovsepyan, and A. Hovhannisyan, Particle bursts from thunderclouds: Natural particle accelerators above our heads, Phys. Rev. D **83**, 062001 (2011).
[6] A. Chilingarian, B. Mailyan, and L. Vanyan, Recovering of the energy spectra of electrons and gamma rays coming from the thunderclouds, Atmos. Res. **114–115**, 1 (2012).
[7] A. Chilingarian and H. Mkrtchyan, Role of the lower positive charge region (LPCR) in initiation of the thunderstorm ground enhancements (TGEs), Phys. Rev. D **86**, 072003 (2012).
[8] A. Chilingarianb, G. Hovsepyan, and L. Kozliner, Thunderstorm ground enhancements gamma ray differential energy spectra, Phys. Rev. D **88**, 073001 (2013).
[9] A. Chilingarian, K. Arakelyan, and K. Avakyan *et al.*, Correlated measurements of secondary cosmic ray fluxes by the Aragats space-environmental center monitors, Nucl. Instrum. Methods Phys. Res., Sect. A **543**, 483 (2005).
[10] G. J. Fishman, P. N. Bhat, R. Mallozzi, J. M. Horack, T. Koshut, C. Kouveliotou, G. N. Pendleton, C. A. Meegan, R. B. Wilson, W. S. Paciesas, S. J. Goodman, and H. J. Christian, Discovery of intense gamma ray flashes of atmospheric origin, Science **264**, 1313 (1994).
[11] A. Chilingarian, S. Chilingaryan, and A. Reymers, Atmospheric discharges and particle fluxes, J. Geophys. Res. **120**, 5845 (2015).
[12] A. Chilingarian, L. Melkumyan, G. Hovsepyan, and A. Reymers, The response function of the Aragats Solar Neutron Telescope, Nucl. Instrum. Methods Phys. Res., Sect. A **574**, 255 (2007).
[13] A. Chilingarian, Thunderstorm ground enhancements: Model and relation to lightning flashes, J. Atmos. Terr. Phys. **107**, 68 (2014).
[14] N. A. Kelley, D. M. Smith, and J. R. Dwyer *et al.*, Relativistic electron avalanches as a thunderstorm discharge competing with lightning, Nat. Commun **6**, 7845 (2015).
[15] http://adei.crd.yerphi.am/adei.
[16] http://wwlln.net.